Published in final edited form as:
Med Phys. 2007 November ; 34(11): 4519–4525.

Improved arterial spin labeling method:

Applications for measurements of cerebral blood flow in human brain at high magnetic field MRI

Geon-Ho Jahng
Department of Radiology, East-West Neo Medical Center, School of Medicine, Kyung Hee University, 149 Sangil-dong, Gangdong-gu, Seoul 134-090, South Korea

Michael W. Weiner and **Norbert Schuff**
Center for Imaging of Neurodegenerative Diseases, Department of Radiology, University of California—San Francisco, 4150 Clement Street, 114M, San Francisco, California 94121

Abstract

Measurements of cerebral blood flow (CBF) with arterial spin labeling (ASL) MRI are challenging primarily due to a poor signal-to-noise (SNR) ratio. Therefore, methods that improve SNR and minimize measurement errors can play a significant role for better estimations of CBF. The purpose of this work was to develop an ASL method for measurements of CBF at high magnetic field strength. In the proposed multislice ASL method, using in-plane double inversion for labeling, stationary spins are kept at equilibrium to avoid T_1 relaxation effects, while blood water is labeled using a lower magnetic field gradient. Improvement for CBF measurements is demonstrated on subjects and by comparison with other multislice ASL MRI methods at 1.5 Tesla. Furthermore, echo-planar imaging (EPI) and Turbo-FLASH (TFL) at 4 T MRI are compared for mapping CBF in human brain using various postlabeling delay times. CBF maps were obtained and analyzed within region-of-interests encompassing either gray matter or white matter. Elimination of T_1 dependence of stationary spins in conjunction with avoidance of magnetization transfer mismatch between labeling and control scans lead to improved CBF measurements. Although measurements of CBF in brain tissue are feasible at 4 T using either EPI or TFL, TFL reduced contaminations from an intravascular signal and susceptibility-related artifacts, providing overall more robust CBF measurements than EPI. Therefore, the proposed ASL method in combination with TFL should be used for measuring CBF of human brain at 4T.

Keywords

arterial spin labeling; cerebral blood flow; high field MRI; in-plane double inversion

I. INTRODUCTION

Measurement of cerebral blood flow (CBF) in human brain is challenging with most imaging techniques for various reasons, including positron emission tomography (PET), dynamic susceptibility contrast (DSC) magnetic resonance imaging (MRI), and arterial spin labeling (ASL) MRI. A main problem of ASL-MRI is a relatively poor signal-to-noise ratio (SNR), because only endogenous blood water is used as the tracer, which comprises only a few percent of the total brain tissue blood water.[1] In addition, the ASL signal is rapidly being diminished due to T_1 relaxation during the arterial transit time (ATT) until blood reaches the capillary bed in brain tissue.[2] Once the spin labels diffuse into the brain, additional signal loss can occur due to interactions of the labels with brain tissue. CBF mapping using echo-planar imaging (EPI) is further complicated by signal loss due to transverse relaxation rate $\left(R_2^*\right)$, which is higher in

brain tissue than in arterial blood.[3] Since R_2^* rates are higher in white matter than gray matter and also increase proportionately with magnetic field strength,[4] the sensitivity of ASL suffers particularly at higher magnetic fields in white matter, although prolonged T_1 relaxation at higher magnetic field strength benefits the ASL signal.[5] Moreover, magnetization transfer (MT) effects between myelin and free water, causing noise and imaging artifacts, can further aggravate problems with CBF mapping, since image voxels may contain different amounts of myelin.

Labeling methods also play an important role for ASL sensitivity. While continuous ASL methods generally provide the highest SNR,[6] they can induce strong magnetization transfer (MT) effects[7] due to the long duration of the radio frequency labeling pulse. In contrast, pulsed ASL methods, such as flow-sensitive alternating inversion recovery (FAIR),[8] or proximal inversion with a control for off resonance effects (PICORE),[9] employ much shorter labeling pulses and thus induce much weaker MT effects,[10] though they may still be measurable. When stationary spins are inverted in both control and labeled schemes as in the FAIR method, they become subject to T_1 relaxations, which may result in subtraction errors. Ideally, stationary spins should remain in equilibrium during ASL in both labeling and control scans to avoid errors related to T_1 relaxation. To maintain stationary spins at equilibrium, the methods of uninverted FAIR (UNFAIR),[11] or equivalently extra-slice spin tagging (EST),[12] were proposed. However, UNFAIR and EST—as initially designed—are limited to single slice selection and moreover work effectively only at exact MR resonance frequency, i.e., for slice in the magnet center.

The overall goal of this study was to improve CBF measurements in human brain by developing pulsed ASL-MRI without T_1 relaxation problems for labeling and reduced dependence on R_2^* and MT. Specifically, the objectives were (1) to design a pulsed labeling scheme which maintains equilibrium of stationary spins in both labeling and control scans and compensates for MT effects while providing multislice imaging capabilities; (2) to combine the proposed ASL scheme with Turbo-Fast low angle shot (FLASH)(TFL) imaging to reduce signal loss due to R_2^*; (3) to compare the sensitivity of TFL with that of EPI to measure CBF of human brain at a high magnetic field strength.

II. METHODS AND MATERIALS

II.A. Proposed arterial spin labeling method

A labeling method, which maintains stationary spins in equilibrium and minimizes MT effects, is shown in Fig. 1. Labeling is achieved by in-plane slice-selective double inversion for both the control and the labeling scans, termed IDOL. For the control scan [*U* in Fig. 1(a)], two inversion pulses [flip angle=π in Fig. 1(a)] of equal amplitude (B_1) and bandwidth are applied in the presence of a magnetic field gradient maintaining equilibrium magnetization for the spins within the imaging region [area 2 in Fig. 1(b)], identical to the spins outside the imaging region [area 1 in Fig. 1(b)] which were not perturbed by labeling. For the labeling scan [*L* in Fig. 1 (a)], again two inversion pulses of equal amplitude (B_1) and bandwidth are applied in the presence of magnetic field gradients, but one of the inversion pulses is now transmitted in the presence of a lower magnetic field gradient. The amplitude of the lower magnetic field gradient is set to excite a slab larger than the imaging region. As a result, spins within the imaging region experiencing double-inversion pulses remain in equilibrium, while spins outside the imaging region, experiencing only a single inversion pulse, are inverted and thus can be differentiated from other spins as they flow into the imaging region. A mismatch of MT is avoided because all inversion pulses are transmitted at the same resonance frequency. Furthermore, since stationary spins within the imaging region remain at equilibrium and therefore are not subject to T_1 relaxation, multislice imaging can be performed across this region without T_1 modulation.

In the absence of T_1 modulation, the control scan yields effectively a proton density image which could be employed in variety of ways, including simultaneous measurements of the blood oxygenation level dependence (BOLD).[9] Moreover, since both control and labeling scans employ slice-selective rf pulses, the velocity dependence of the ASL signal is the same for control and labeling scans, thus reducing velocity modulations upon subtracting the two scans as shown later below [area 3 in Fig. 1(b)].

II.B. Comparisons between IDOL and UNFAIR or FAIR

IDOL was combined with a multislice gradient-echo EPI sequence, implemented on a 1.5 T MRI system (Siemens, Vision) and tested on five healthy volunteers. Figure 1(c) shows the schematic drawing of the pulse sequence. Following labeling with IDOL after a period TI1, 14 periodic saturation pulses were applied within a 20 mm band distal to the imaging region, as shown in Fig. 1(b), to destroy any magnetization trailing the inflowing labeled blood, thus avoiding dilution of the ASL signal from unlabeled spins during imaging.[13] Following the saturation pulses, a multislice gradient-echo EPI sequence (seven slices, each 8 mm thick with a 2 mm gap between slices; 4×2 mm^2 in-plane resolutions) with a sinc-shaped rf pulse for slice excitation (90 deg) was used for perfusion-weighted imaging (PWI). For comparison, labeling with IDOL was replaced by UNFAIR/EST and FAIR ASL methods while the rest of the sequence remained the same. *TR*/*TE*=3000/15 ms was used in all experiments. Two principally different conditions were tested: (1) Labeling without subsequent periodic saturation for a total postlabeling delay (TI_2) of 1600 ms; (2) Labeling followed after 800 ms (TI_1) by period saturation pulses for a total postlabeling delay of again 1600 ms. Scan time for 32 averages was 3 min.

II.C. Comparisons between EPI and TFL for IDOL

IDOL was combined with either gradient-echo EPI (EPI-IDOL) or TFL (TFL-IDOL) for mapping CBF in human brain. The sequences were implemented on a 4 T MRI system (Bruker/Siemens, MedSpec) and tested on eight healthy volunteers (mean age=48 years, range 27 to 57 years, six men and two women). To test the effect of arterial transit delays on CBF mapping, ASL images were acquired at different postlabeling delay times (TI_2) varying from 1200 to 3000 ms in steps of 300 ms. The acquisition parameters of EPI were *TR*=3500 ms, *TE*=9 ms, matrix=48×64, voxel size=4×4×6 mm with 1.5 mm gap, number of slices=9, number of measurements=60; and those of TFL were *TR*=155 ms (time from the first excitation pulse to the last acquisition), *TE*=2.28 ms, flip angle=10 deg with centric reordering and rf spoiling, bandwidth=320 Hz/pixel, and ascending slice order. The rest of the parameters for IDOL preparation were the same in EPI and TFL. Measurement times for each image frame were 3.34 min for EPI-IDOL and 4.30 min for TFL-IDOL. IDOL labeling and control scans were subtracted to obtain PWI data. The PWI data were converted into parametric CBF maps for *each* TI_2 delay time using a single compartment and instant equilibrium model for a blood tracer,[14]

$$\Delta M = 2M_{0t} \cdot \mathrm{CBF} \cdot \frac{\alpha}{\lambda} \cdot TI_1 \cdot e^{(-TI_2/T_{1b})} \cdot E. \quad (1)$$

Here, ΔM is the perfusion weighted signal, M_{ot} is the control scan signal, CBF is in units of ml/100g/min. α(0.95) and λ(ml/100 g) describe the labeling efficiency and the tissue-to-blood partition, respectively. For simplicity, it was assumed that both parameters are unity. TI_1 (800 ms or 0.013 min) is the interval between the middle of the inversion pulse and the start of the periodic saturation pulse train and TI_2(ms) is the period between the inversion pulse and the excitation pulse. By definition, TI_2 is a function of the slice order as blood flow advances from the labeling gap to the distal slice position in the brain, hence $TI_2(n)=TI_2+n*Tx$. Here, n is the slice order and Tx is the imaging time of EPI or TFL. T_{1b}(ms) is the longitudinal relaxation time of blood. E is a correction factor to account for potential scaling of longitudinal relaxation

times of brain tissue (T_{1t}) and blood (T_{1b}) as a consequence of rapid rf pulse readout of the ASL signal. Hence, E is dependent on the sequence. Initially, E=1 is assumed (see Sec. IV for further details on E).

II.C.1. Postprocessing—Processing of the ASL data was performed off-line and included the following steps using the Statistical Parametric Mapping version 2 (SPM2) software [http://www.fil.ion.ucl.ac.uk/spm/software/spm2/]:

Step 1 (Alignment): The 60 PWI data sets of each TI_2 were aligned to each other and a mean image generated, separately for each subject and sequence (EPI or TFL), using rigid body affine registration to minimize motion artifacts between measurements.

Step 2 (Calculation of PWI and CBF maps): Home-written code in MATLAB software was used to convert each mean PWI set from step 1 to a parametric CBF map, according to Eq. (1). The first two data points of each TI_2 set had to be ignored in the calculation because of artifacts due to T_1.

Step 3 (Co-registration): For each sequence, the mean PWI sets of each subject were then co-registered to the corresponding anatomical MRI data [three dimensional (3D) T_1-weighted images with 1×1×1 mm resolution, 2 s inversion time] of each subject using a mutual information technique available in SPM.

Step 4 (Spatial normalization): Nonlinear spatial normalization of the CBF maps was achieved by first registering the anatomical T_1-weighted images of the volunteers to a T_1 brain template and then applying the same transformation parameters, adjusted for resolution, to the CBF maps of each subject. Finally, the CBF maps were resliced and interpolated to 2×2×2 mm voxel size for region of interest analysis (ROI).

Step 5 (Regions-of-interest ROI definitions): Three ROIs were selected, each in anterior (AC) and posterior (PC) cingulate cortex, representing gray matter regions and another ROI in the central semiovale, representing white matter region. The spatially normalized anatomical 3D T_1-weighted image of all subjects in conjunction with MRICRO software [http://www.sph.sc.edu/comd/rorden/mricro.html] was used to guide ROI placement. Mean values of signal intensity (SI) of control and labeled images and CBF values were computed for each ROI, separately for each sequence, TI_2 delay time and subject. *S*-PLUS software (Insightful Corporation, Seattle, WA) was used for statistical analysis. Comparisons were evaluated using *t*-tests with alpha=0.05 as level of significance.

III. RESULTS

III.A. Comparisons between IDOL and UNFAIR or FAIR

Figure 2 shows representative PWI data from a volunteer obtained using either IDOL, FAIR, or UNFAIR without [Fig. 2(a)] and with [Fig. 2(b)] application of periodic saturation pulses. Similar data were obtained from the other four volunteers. The data show: (1) IDOL yielded better image uniformity across slices than UNFAIR [Figs. 2(a) and 2(b)], consistent with improved labeling scheme using slice-selective double inversions; (2) IDOL also showed less signal contamination from large blood vessels than UNFAIR and FAIR, as seen in Figs. 2(a) and 2(b). Furthermore, IDOL in combination with period saturation pulses reduced flow artifacts in PWI data, presumably because IDOL is less sensitive to velocity variations of inflowing blood than FAIR [Fig. 2(b)]. Specifically, IDOL was largely immune to changing the number of saturation pulses, whereas image quality degraded quickly in FAIR when the number of saturation pulses was reduced. UNFAIR, which uses double inversion similar to IDOL, was also relatively immune to varying the number of saturation pulses.

III.B. Comparisons between EPI and TFL for IDOL

Figure 3 shows spatially normalized representative CBF maps from a volunteer obtained with EPI [Fig. 3(a)] and TFL [Fig. 3(b)] readouts at TI_2=2400 ms. Note the CBF maps were calculated for each TI_2 value and show a high gray/white contrast. Overall, CBF maps were less variable with TFL acquisition than with EPI. .

Figure 4(a) shows mean signal intensities (SI) and standard deviations of raw control and labeled images averaged over all eight subjects as a function of the postlabeling delays time (TI_2), separately for each ROI and for each sequence (EPI or TFL). Mean signal intensities acquired with EPI were higher than those acquired with TFL for all three ROIs (p<0.0001 for AC, p<0.0004 for PC, and p<0.0001 for WM by t-tests). As expected, the mean signal intensities in white matter were lower than those in gray matter for both EPI (p<0.002) and TFL (p<0.052). For TFL, the mean signal intensity in the posterior cingulate was higher than that in the anterior cingulate, though the difference was not significant (p=0.38). In contrast, EPI yielded a substantially lower signal intensity in the posterior cingulate than in the anterior cingulate (p<0.0001).

Figure 4(b) shows mean CBF values and standard errors from data of the eight volunteers obtained in three ROIs and calculated for individual TI_2 time. Note, CBF was computed separately for each TI_2 time delay to assess the variability of the CBF measurements, which should theoretically be independent of TI_2 . In EPI, CBF values in the anterior cingulate systematically varied as a function of TI_2 times, indicating a measurement bias toward shorter TI_2 . CBF values from EPI were also higher than those from TFL for all three ROIs (p=0.0006 for AC, p=0.001 for PC and p=0.048 for WM). TFL yielded higher CBF in the posterior cingulate than in the anterior cingulate (p=0.043), while EPI yielded the opposite (p<0.023). CBF values in white matter for both EPI and TFL systematically increased up to TI_2=2100 ms and then flattened or decreased, which may reflect a much longer arterial transit time of white matter than of gray matter.

Table I lists coefficients of variation (CoV, standard deviation divided by the mean) of signal intensities of control and labeled images in the three ROIs, separately for EPI and TFL. Signal variability was significantly lower in TFL than EPI in all three ROIs (P<0.0001 for AC, p<0.0004 for PC, and P<0.0001 for WM). In contrast to signal intensity, the CoV values were not significantly different between TFL and EPI. CoV values for CBF of white matter were significantly higher than those of gray matter for both EPI (p<0.0008) and TFL (p<0.0006).

IV. DISCUSSION

We implemented a new ASL method in combination with multislice image acquisition and demonstrated improved spin labeling properties on a 1.5 and a 4 T MRI system. In addition, we compared CBF measurements between 1.5 and 4 T as well as between gradient-echo EPI and TFL imaging at 4 T. Compared to FAIR, IDOL provided more consistent CBF measurements, likely because of a combination of greater immunity to variations in blood velocity and elimination of T_1 differences between control and labeling scans. Compared to UNFAIR, IDOL was less confounded by signal nonuniformity across slices by improving balance of rf and gradient pulse between labeling and control scans. However, other ASL methods, such as pseudo-continuous[15] or TILT,[16] may also improve MT. In general, it is expected that perfusion yields a uniform pattern of signal variation for ASL and systematic modulations are the result of induced artifacts. Therefore, signal nonuniformity across slices may be a useful indicator for the performance of ASL methods. In this study for example, both the FAIR and UNFAIR methods yielded a higher signal for bottom and top slices than for slices in the middle, as seen in Fig. 2, indicating a systematic measurement error. MT effects and contamination of the perfusion signal from residual intravascular labeled blood water can

be responsible for signal nonuniformities across slices. An ASL method that yields more signal uniformity across slices could therefore be considered superior to methods that lead to large nonuniformity.

IDOL was combined with two different mapping techniques, EPI and TFL, to assess the impact of R_2^* on CBF measurement at higher magnetic field strength. Although EPI yielded a higher PWI signal than TFL and correspondingly, higher CBF values, measurement variability, expressed as CoV, was markedly lower for TFL than for EPI. A higher yield of the ASL signal for EPI, but less measurement variability for TFL, suggests that each method is associated with a systematic bias. There are several explanations for this outcome: First, the ASL signal (subtraction of the labeled image from the unlabeled image) may be reduced in TFL because contributions from blood vessels are better suppressed by the multiple excitation rf pulses of TFL than by the single excitation pulse of EPI. In EPI, the ASL signal may therefore be more contaminated by contributions from blood vessels than in TFL, leading to a higher ASL signal and an overestimation of CBF with EPI. The contamination of the ASL signal may also explain the low variability of CBF measurements with EPI. Several previous ASL studies showed that CBF value acquired with EPI tend to increase if no diffusion gradient[17] or a long postlabeling delay[18] were used to suppress contributions from large vessels. Second, another explanation for lower CBF values in TFL than EPI may be related to assumptions made when modeling CBF. Parametric models of CBF usually assume E=1, in Eq. (1), ignoring sequence-dependent scaling of relaxation rates due to rapid rf repetitions. The expression for E is[14]

$$E=\frac{e^{(-\delta R_1 \cdot T_{1b})}-1}{\delta R_1 \cdot TI_1}, \tag{2}$$

where $\delta R_1=R_{1b}-R_{1app}$. $R_{1b}(=1/T_{1b})$, $R_{1app}(=R_{1t}+f/\lambda)$, and R_{1t} are the longitudinal relaxation rates of blood, brain tissue with flow, and brain tissue, respectively. For rf pulse repetition rates much higher than $1/T_1$, the longitudinal relaxation time scales according to $T_1^*=TR_\beta/\left(TR_\beta/T_1-\ln(\cos[\beta])\right)$, where β is the tip angle and TR_β is the repetition time between the β pulses. For TFL of this study, T_1^* accordingly should shorten to 0.939 s from 1.35 s for gray matter and to 0.72 s from 0.939 s (Ref. 19) for white matter. Hence, CBF differences between EPI and TFL should be reduced if the T_1^* scaling due to rapid rf pulsing is considered. With consideration of T_1^*, the average CBF values of PC gray matter becomes 55.6±21.9 ml/100 g/min for EPI and 47.3±16.1 ml/100 g/min for TFL. Similarly, the average CBF value of white matter with the T_1^* correction becomes 19.3±9.1 ml/100 g/min for EPI and 16.5±7.5 ml/100 g/min for TFL. Therefore, when we correct the E-factor, the differences of CBF values between EPI and TFL acquisitions are reduced. We expected the ratio of CBF of white matter to gray matter to be higher for TFL than for EPI because signal loss due to T_2^* decay is more prominent for EPI than for TFL. However, the ratio of CBF of white matter to gray matter, i.e., posterior cingulate, was approximately 0.3, regardless of EPI or TFL readouts. The ratio is similar to that of simulations from another study, but smaller than results from studies using radioactive tracers.[20] In the present study, we used the minimum TE=9 ms with half Fourier and partial k-space acquisition for EPI. The T_2^* effect can maximize the TE of about 40 ms at a 4 T MRI. The observation that both EPI and TFL yielded the same ratio of white to gray matter CBF implies that higher R_2^* of white matter at 4 T MRI is not the main source of error for EPI. In addition, white matter CBF values currently obtained with an ASL-MRI technique are currently of limited use because of intrinsically low SNR in white matter compared to that in gray matter. New developments of ASL-MRI are necessary to obtain more reliable CBF values of white matter. Previous ASL-MRI has primarily focused on reproducibility of ASL in gray matter,[21] while few studies investigated reproducibility of ASL in white matter. In the future, studies on a larger and more heterogeneous group of subjects need to be performed to determine reproducibility of CBF measurements in white matter using ASL MRI.

V. CONCLUSIONS

An improved ASL method has been introduced that eliminates dependence of T_1 fluctuations of stationary spins and reduces MT artifacts while permitting multislice perfusion imaging. Compared to other ASL methods, the improved approach is more robust and therefore should improve accuracy in measuring regional CBF. Feasibility to measure CBF in human brain at 4 T was demonstrated for both EPI and TFL acquisitions. Although EPI yielded a higher ASL signal, TFL was less confounded by an intravascular signal and more immune to magnetic susceptibility effects. Therefore, IDOL in combination with TFL is recommended for measuring brain perfusion at high magnetic fields.

ACKNOWLEDGMENTS

The authors thank Dr. Antao Du and Dr. Susanne Muller at the University of California San Francisco for advising postprocessing the ASL data, and Dr. Chang Ho Ryu at the Kyung Hee University for identifying the regions-of-interesting (ROIs) on MRI. We also thank Dr. John Kornak at the University of California San Francisco for guidance in statistical analyses. This study was supported by a grant of the Korean Health 21 R&D Project, Ministry of Health & Welfare, Republic of Korea (A062284).

References

1. Herscovitch P, Raichle ME. What is the correct value for the brain-blood partition coefficient for water? J. Cereb. Blood Flow Metab 1985;5:65–69. [PubMed: 3871783]
2. Yang Y, Engelien W, Xu S, Gu H, Silbersweig DA, Stern E. Transit time, trailing time, and cerebral blood flow during activation: Measurement using multislice, pulsed spin-labeling perfusion imaging. Magn. Reson. Med 2000;44:680–685. [PubMed: 11064401]
3. Haacke, EM.; Brown, RW.; Thompson, MR.; Venkatesan, R. Magnetic Resonance Imaging: Physical Principles and Sequence Design. Wiley & Sons; New York: 1999.
4. Haacke EM, Cheng NY, House MJ, Liu Q, Neelavalli J, Ogg RJ, Khan A, Ayaz M, Kirsch W. Imaging iron stores in the brain using magnetic resonance imaging. Magn. Reson. Imaging 2005;23:1–25. [PubMed: 15733784]
5. Kruger G, Glover GH. Physiological noise in oxygenation-sensitive magnetic resonance imaging. Magn. Reson. Med 2001;46:631–637. [PubMed: 11590638]Golay X, Petersen ET. Arterial spin labeling: Benefits and pitfalls of high magnetic field. Neuroimaging Clin. N. Am 2006;16:259–268. [PubMed: 16731365]
6. Wang J, Alsop DC, Li L, Listerud J, Gonzalez-At JB, Schnall MD, Detre JA. Comparison of quantitative perfusion imaging using arterial spin labeling at 1.5 and 4.0 Tesla. Magn. Reson. Med 2002;48:242–254. [PubMed: 12210932]
7. Williams DS, Detre JA, Leigh JS, Koretsky AP. Magnetic resonance imaging of perfusion using spin inversion of arterial water. Proc. Natl. Acad. Sci. U.S.A 1992;89:212–216. [PubMed: 1729691]
8. Kim SG. Quantification of relative cerebral flow change by flow-sensitive alternating inversion recovery (FAIR) technique: Application to functional mapping. Magn. Reson. Med 1995;34:293–301. [PubMed: 7500865]
9. Wong EC, Buxton RB, Frank LR. Implementation of quantitative perfusion imaging techniques for functional brain mapping using pulsed arterial spin labeling. NMR Biomed 1997;10:237–249. [PubMed: 9430354]
10. Wolff SD, Balaban RS. Magnetization transfer contrast (MTC) and tissue water proton relaxation in vivo. Magn. Reson. Med 1989;10:135–144. [PubMed: 2547135]Pekar J, Jezzard P, Roberts DA, Leigh JS Jr. Frank JA, McLaughlin AC. Perfusion imaging with compensation for asymmetric magnetization transfer effects. ibid 1996;35:70–79.
11. Helpern JA, Branch CA, Yongbi MN, Huang NC. Perfusion imaging by uninverted flow-sensitive alternating inversion recovery (UNFAIR). Magn. Reson. Imaging 1997;15:135–139. [PubMed: 9106140]
12. Berr SS, Mai VM. Extraslice spin tagging (EST) magnetic resonance imaging for the determination of perfusion. J. Magn. Reson. Imaging 1999;9:146–150. [PubMed: 10030662]

13. Luh WM, Wong EC, Bandettini PA, Hyde JS. QUIPSS II with thin-slice TI1 periodic saturation: A method for improving accuracy of quantitative perfusion imaging using arterial spin labeling. Magn. Reson. Med 1999;41:1246–1254. [PubMed: 10371458]

14. Buxton RB, Frank LR, Wong EC, Siewert B, Warach S, Edelman RR. A general kinetic model for quantitative perfusion imaging with arterial spin labeling. Magn. Reson. Med 1998;40:383–396. [PubMed: 9727941]

15. Garcia DM, de Bazelaire C, Alsop D. Pseudo-continuous Flow Driven Adiabatic Inversion for Arterial Spin Labeling. Proc. Intl. Soc. Magn. Reson. Med., Miami Beach 2005:37.

16. Golay X, Stuber M, Pruessmann KP, Meier M, Boesiger P. Transfer insensitive labeling technique (TILT): Application to multislice functional perfusion imaging. J. Magn. Reson. Imaging 1999;9:454–461. [PubMed: 10194717]

17. Wang J, Alsop DC, Song HK, Maldjian JA, Tang K, Salvucci AE, Detre JA. Arterial transit time imaging with flow encoding arterial spin tagging (FEAST). Magn. Reson. Med 2003;50:599–607. [PubMed: 12939768]

18. Donahue MJ, Lu H, Jones CK, Pekar JJ, van Zijl PC. An account of the discrepancy between MRI and PET cerebral blood flow measures: A high-field MRI investigation. NMR Biomed 2006;19:1043–1054. [PubMed: 16948114]

19. Kim SG, Hu X, Ugurbil K. Accurate *T*1 determination from inversion recovery images:Application to human brain at 4 Tesla. Magn. Reson. Med 1994;31:445–449. [PubMed: 8208121]

20. Ye FQ, Berman KF, Ellmore T, Esposito G, van Horn JD, Yang Y, Duyn J, Smith AM, Frank JA, Weinberger DR, McLaughlin AC. H(2)(15)O PET validation of steady-state arterial spin tagging cerebral blood flow measurements in human. Magn. Reson. Med 2000;44:450–456. [PubMed: 10975898]

21. Jahng GH, Song E, Zhu XP, Matson GB, Weiner MW, Schuff N. Human brain: Reliability and reproducibility of pulsed arterial spin-labeling perfusion MR imaging. Radiology 2005;234:909–916. [PubMed: 15734942]Ewing JR, Cao Y, Knight RA, Fenstermacher JD. Arterial spin labeling: Validity testing and comparison studies. J. Magn. Reson. Imaging 2005;22:737–740. [PubMed: 16261575]Yen YF, Field AS, Martin EM, Ari N, Burdette JH, Moody DM, Takahashi AM. Test-retest reproducibility of quantitative CBF measurements using FAIR perfusion MRI and acetazolamide challenge. Magn. Reson. Med 2002;47:921–928. [PubMed: 11979571]

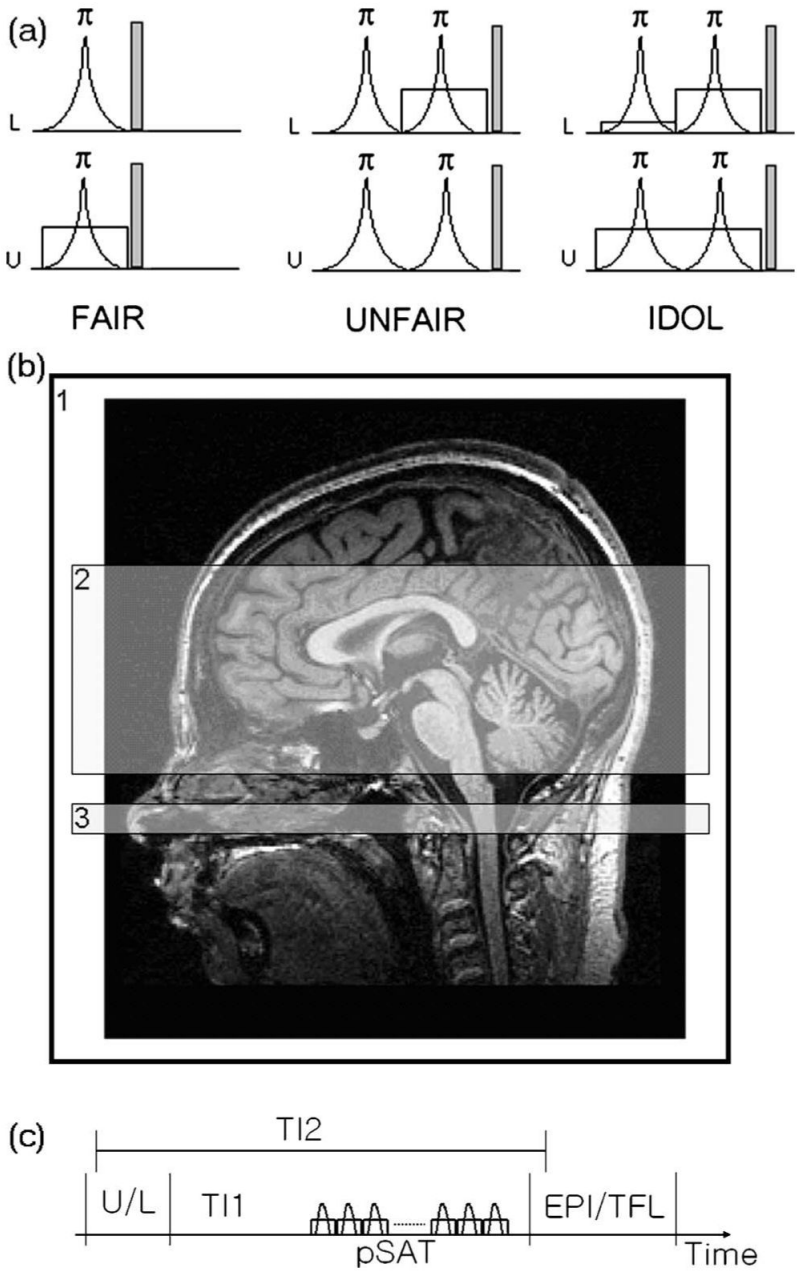

FIG. 1.

Three types of pulsed arterial spin labeling methods (a) with imaging position (b). (a) Labeled (*L*) and unlabeled (*U*) schemes of FAIR, UNFAIR, and the proposed method (IDOL). A radio frequency pulse was shown in a curve, representing the inversion pulses with flip angle of 180 deg. A spoiler gradient was applied after rf pulses to minimize a residual magnetization. A slice-selective gradient was represented by a rectangular shape. The amplitude of the first small gradient was decided by the size of the used head coil. (b) Locations of labeling by using an entire head coil (area 1) used in the first slice-selective gradient of the labeling (*L*) in the IDOL, imaging (area 2) used in other slice-selective gradient in all three methods, and the periodic saturation pulse (area 3). (c) The schematic drawing of the pulse sequence. pSAT is the periodic saturation pulses applied in area 3 in (b).

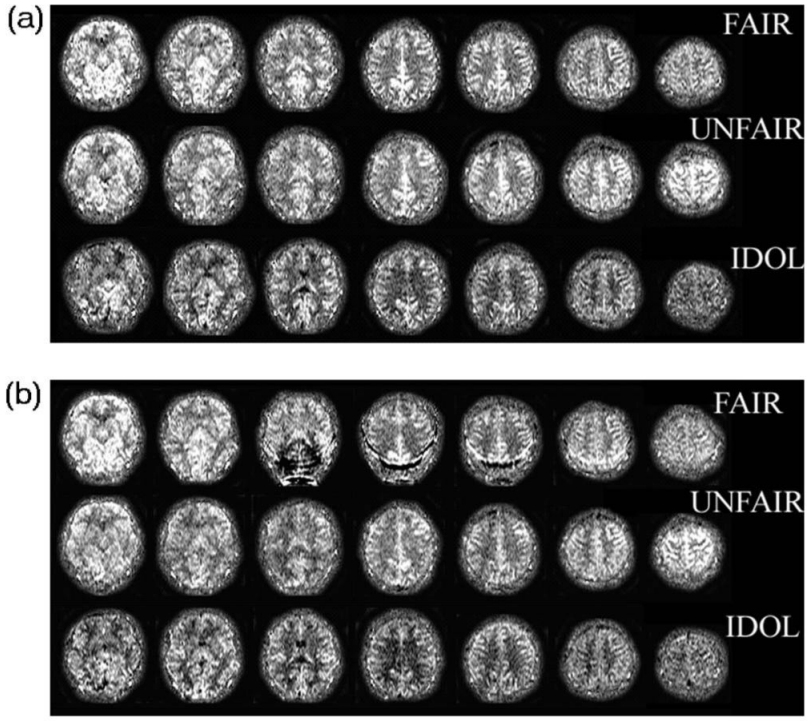

FIG. 2.

Inflow dependency and magnetization transfer (MT) effect in perfusion weighted imaging (PWI) of three pulsed arterial spin labeling methods to evaluate signal fluctuations by varying the periodic saturation pulses at the total postlabeling delay time TI_2 of 1600 ms at a 1.5 T MRI. The proposed IDOL method is improved in MT effect and is insensitive signal fluctuations. (a) PWI acquired without periodic saturation; (b) PWI acquired with periodic saturation (TI_1=800 ms).

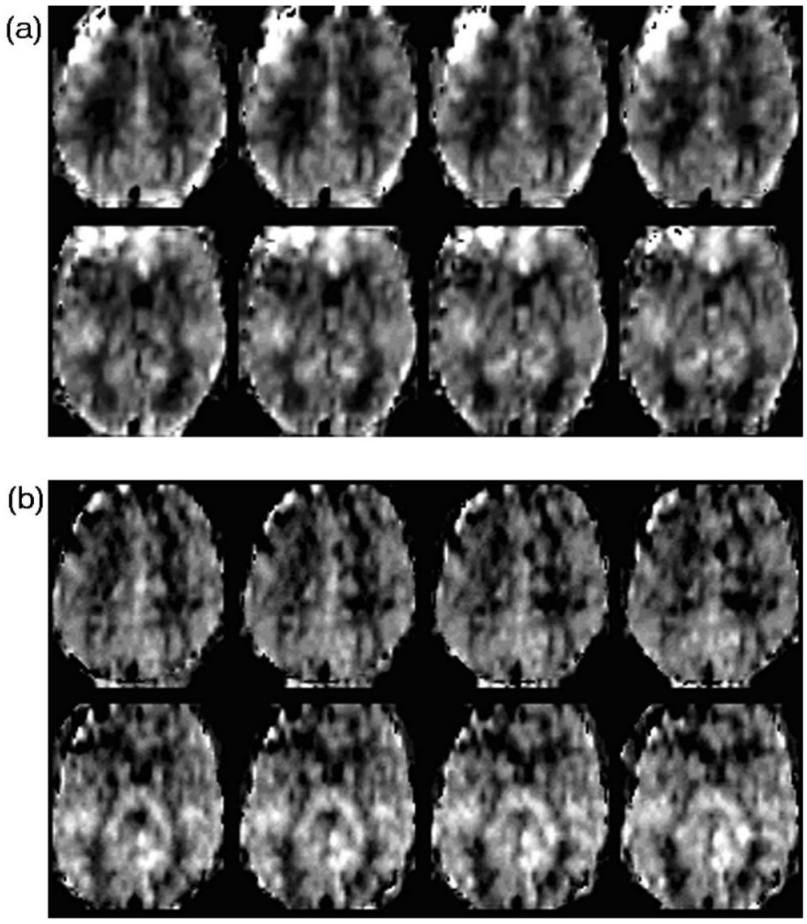

FIG. 3.

A representative cerebral blood flow (CBF) maps obtained from a volunteer acquired with the proposed method with an echo planner imaging (EPI) sequence and a Turbo-FLASH (TFL) sequence at the total post labeling delay time TI_2 of 2400 ms at a 4 T MRI. CBF values at the frontal lobe acquired with EPI sequence are systematic errors, but not with TFL sequence. (a) CBF maps acquired with a gradient-echo EPI sequence. (b) CBF maps acquired with a TFL sequence.

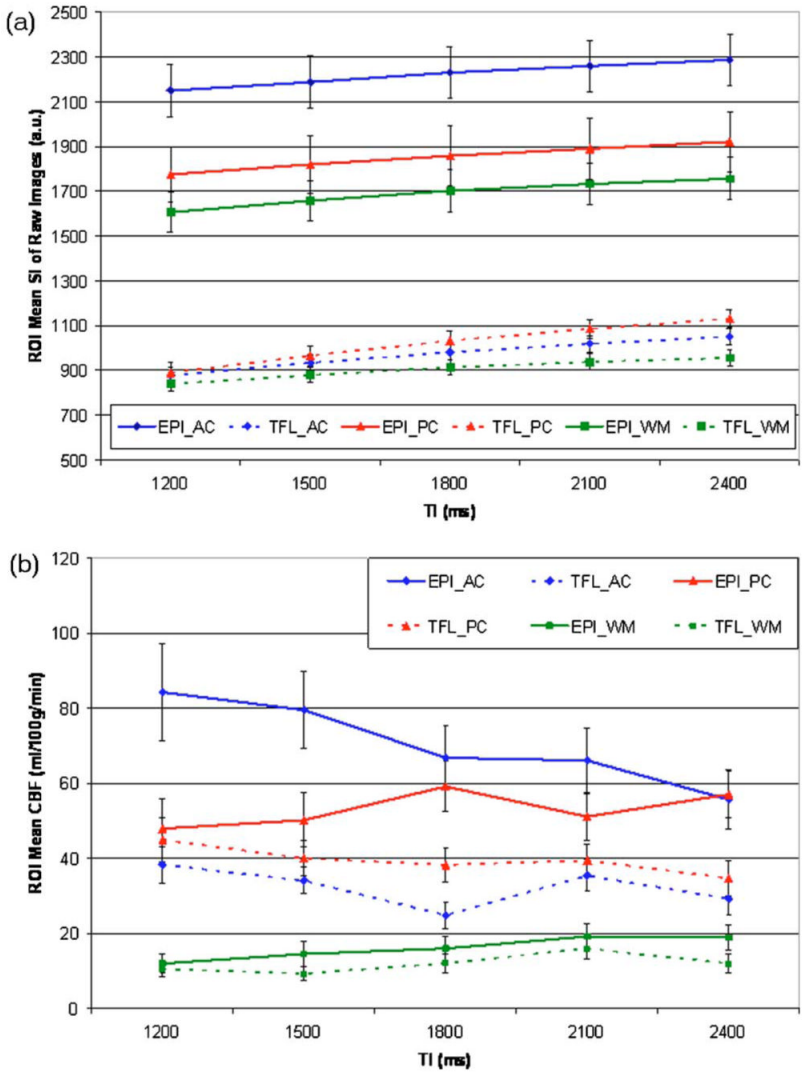

FIG. 4.

Mean changes for the three regions-of-interest (ROI) and for the two sequences as a function of the postlabeling delays time (TI_2) averaged over eight volunteers. Three ROIs are anterior cingulate (AC), posterior cingulate (PC), and central semiovale (WM). (a) Mean signal intensities (SI) and the corresponding standard deviation (STD) of raw control and labeled images for three ROIs over eight volunteers. (b) Mean cerebral blood flow (CBF) values with the standard errors (STD/square root of number of volunteers) obtained in three ROIs and calculated for individual postlabeling delay time (TI_2) over eight volunteers.

TABLE I

Coefficient of variation (CoV, standard deviation divided by mean) of signal intensities (SI) of raw control and labeled images for each TI_2 in the three regions-of-interest (ROI) acquired with the proposed method with a gradient-echo echo planner imaging (EPI) readout and a Turbo-FLASH (TFL) readout at the 4 T MRI. AC: anterior cingulate; PC: posterior cingulate; WM: central semiovale

	CoV(%) of each TI_2 (ms) for EPI Readouts				
ROI	**TI_2=1200 ms**	**TI_2=1500 ms**	**TI_2=1800 ms**	**TI_2=2100 ms**	**TI_2=2400 ms**
SI_AC	5.47	5.32	5.18	5.07	5.11
SI_PC	7.04	7.09	7.33	7.31	7.08
SI_WM	5.48	5.38	5.48	5.36	5.36

	CoV(%) of each TI_2 (ms) for TFL Readouts				
ROI	**TI_2=1200 ms**	**TI_2=1500 ms**	**TI_2=1800 ms**	**TI_2=2100 ms**	**TI_2=2400 ms**
SI_AC	4.04	3.76	3.56	3.51	3.51
SI_PC	5.17	4.63	4.22	3.85	3.48
SI_WM	3.52	3.68	3.84	3.93	4.03